CHAPTER 5

PERFORMANCE IMPROVEMENT OF GRID-LESS RELTRON

CHAPTER 5

PERFORMANCE IMPROVEMENT OF GRID-LESS RELTRON

5.1. Overview

In recent years, extensive research activities have been aroused in the domain of the power enhancement of high-power microwave (HPM) oscillators. Therefore, in this chapter, a new variant of the reltron oscillator i.e. grid-less reltron with explosive emissive cathode has been proposed for high microwave power generation and long RF pulse generation. The EM behavior and RF behavior of the proposed variant are investigated through a commercial code "CST Studio Suite". The electric field distribution and resonant frequency corresponding to the different resonance modes of the SCC have been obtained using the eigenmode solver and the frequency domain solver, respectively. The RF behavior of the proposed variant has been investigated using CST's PIC solver. Also, the effect of different electrical parametric on the RF output power, efficiency, and RF pulse-width have been investigated. The simulation results predicted that the proposed variant of reltron is capable to produce an RF pulse of peak power of ~200 MW and a pulse width of 1 μs with an efficiency of ~41%. The simulation results of the proposed variant have been compared with the experimental reported results of gridded and grid-less reltron. Simulation results show that the proposed variant generates approximately the peak RF output power equivalent to a gridded reltron with a low operating supply and the width of the generated RF signal is also 10 times higher than that of a gridded reltron. While when this variant is compared to the grid-less reltron it generates an RF peak power 10 times higher than the grid-less reltron but the generated RF pulse width is 1/5 times lower than the gridded reltron.

5.2. Introduction

The research activities to enhance the RF output power have been significantly increased in the domain of high power microwave (HPM). To improve the RF output power generally, the researcher focussed to modify the design of the key assemblies (i.e. RF interaction cavity, cathode section, extraction section, and collector section) of the device [Bromborsky *et al.* (1987), Krall *et al.* (1991), Tau *et al.* (2004), Lin and Liu (2011), Xiao *et al.* (2011), Jiang *et al.* (2015)]. Another approach to enhance the RF output power is to combine the RF output power of several similar or different HPM sources spatially. Many experiments proved that integrating the microwave power of multiple phase-locking microwave sources is the promising approach to achieve high microwave power [Benford *et al.* (1989), Teng *et al.* (2012), Lian *et al.* (2014), Xiao *et al.* (2014)].

A highly efficient gridded reltron was experimentally reported by Titan Advanced Innovative Technologies of Albuquerque, NM in the year 1992. The initial experimental results show that for L-band with the applied DC input voltage of 800 kV and an average input beam current of 1.2 kA the device generates a peak RF power of >400 MW with the peak conversion efficiency of ≥50%. The total RF energy per pulse for 375 MW peak RF power was 84 J. The transparency of the stainless steel screens or grid used within the RF interaction cavity was considered over 95%. For the S-band, the device generated a peak RF power of 235 MW with a peak conversion efficiency of ~40% when the DC input voltage of 850 kV and an average input beam current of 750 A was applied. The electron bunching mechanism of the device was based on virtual cathode formation and it did not require any external DC magnetic field for guiding the electron beam [Miller *et al.* (1992)].

In the year 1994, Miller *et al.* reported the analytical model for the rectangular extraction cavity to optimize the extraction of the RF output power and obtained a frequency tunning ability in the device by physically deforming the RF interaction cavity by plungers and tunning screws. This tuning feature was built outside the Marx generator tank to achieve this frequency tunability without disassembling the tube or losing the vacuum. For the L-band, a peak RF power of ~600 MW and an RF energy per pulse >200 J were obtained, whereas the tunable version of reltron is reported in the S-band. The tunable version of the reltron was capable to generate the peak RF power of >350 MW and the conversion efficiency ~50%. In achieving the ± 5% frequency tunability from the center frequency of the reltron, the peak RF output power was reduced by about 3 dB and this fall in power can be minimized by increasing the injector voltage. They also demonstrate the multiple frequency operation by using an S-band output cavity with an L-band reltron [Miller *et al.* (1994)]. Miller *et al.* also discussed experimental results and theoretical design considerations of the reltron source for three specific issues: long pulse operation, extended frequency operation, and extended lifetime designs. For long pulse and high PRR operation, they developed a new variant of reltron (i.e. grid-less reltron) which uses thermionic cathodes, ceramic insulators, and grid-less RF interaction cavity for extended lifetime operation at reasonably high average power levels (>100 kW) [Miller *et al.* (1995)]. The electron bunching mechanism of the grid-less reltron is based on double velocity modulation and it requires a small external DC magnetic field for guiding the electron beam. The experimentally reported grid-less reltron generates a 20 MW RF peak power signal for 5 μs with 40% efficiency. This device is well suited for high-average-power applications and having a high repetition rate i.e. ≥100 Hz. Since the grid-less reltron uses a metal disc rather than metal grids in the RF interaction cavity, therefore it does not

require regular maintenance just like a gridded reltron. Because in gridded reltron metal grid, which is used in RF interaction cavity get damaged after a few shots and requires replacement of grids at regular time intervals for its proper operation [Miller *et al.* (1995)].

To enhance the RF output power of the reltron oscillator, Soh *et al.* reported a simulation study of the dual cavity gridded reltron. In this research work, instead of a single RF interaction cavity, two RF interaction cavity was used in reltron and the second RF interaction cavity was used to enhance the beam modulation [Soh *et al.* (2011)]. The enhanced beam modulation helps in the formation of more tight electron bunches as compared to the single cavity-based reltron. As a result of this, the dual cavity reltron generates more RF output power as compared to a single cavity reltron. Kim *et al.* reported a simulation-study of grid-less reltron in which high post-acceleration DC voltage was used to enhance the RF output power [Kim *et al.* (2009)]. The RF output power is increased about two times as compared to the reported grid-less reltron, but the pulse width of the RF signal is reduced by 25 times and this pulse reduction is due to the pulse shortening phenomenon. The use of high post acceleration voltage is the main reason behind the pulse shortening in this device.

In this chapter, a new variant of the reltron oscillator has been proposed to take advantage of both types of reltron oscillators, the device equipped with the ability to produce higher RF output power similar to the gridded reltron, and the longer RF pulse width just similar to the grid-less reltron. Since the proposed device is free from metal grids, therefore, the possibility of achieving higher PRR with the proposed version is much more. Another advantage of not using metal grids is that the chances of plasma formation in the vicinity of metal grids greatly is reduced, therefore eliminates the problem of replacement of grids at regular intervals. The proposed variant of the reltron oscillator

operates with the annular explosive emission cathode with the grid-less reltron configuration. The comprehensive simulation studies have been performed before its practical testing because simulation studies play an important role in order to save the experimental testing cost of any instrument. Simulation studies, also very helpful in identify key parameters of the device that affect the RF output power and efficiency of the device. Apart from all this, the simulation study also helps in developing a better understanding of the beam wave interaction mechanism of the RF interaction cavity and the RF behavior of the device. Therefore, to achieve the goal, an extensive simulation study has been performed to know the RF behavior of the proposed variant.

5.3. Simulation Study

A 3D schematic view of the proposed variant of reltron is shown in Fig. 5.1. The geometry of the proposed variant of reltron consists of a cathode section, RF interaction cavity, post acceleration region, and extraction section. To generate the electron beam, an annular explosive emissive cathode model is selected. The annular explosive emissive cathode has been chosen instead of the solid explosive emissive cathode because the annular explosive emissive cathode is capable of generating more beam current than the solid explosive emissive cathode. Another reason for selecting the annular cathode rather than the solid cathode is that it requires a 15% lower uniform guiding magnetic field than the solid cathode and it also avoids the high-temperature requirement, complicated electron-optical system, large area convergence, high current density, and emission uniformity for the solid beam [Zhu *et al.* (2015)].

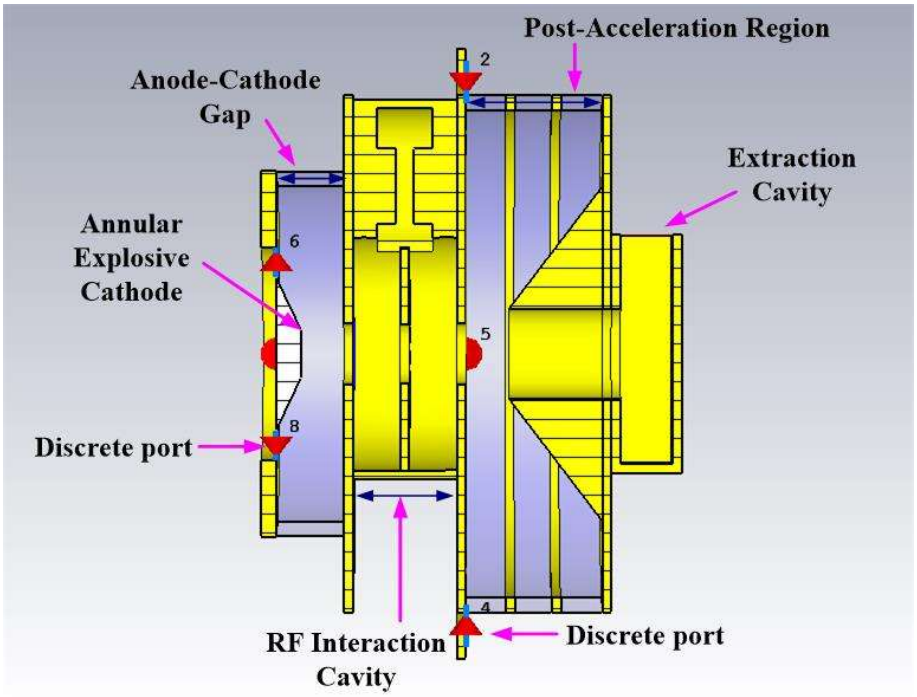

Figure 5.1: 3D schematic of the proposed variant of reltron.

The working principle of the proposed variant is similar to the grid-less reltron i.e. double velocity modulation of the electron beam [Miller *et al.* (1992)]. The generated continuous electron beam from the annular explosive cathode is converted into the discrete bunches of the electron with the help of the RF interaction cavity. This multi-cavity resonating system i.e. SCC resonates at 0-mode, π/2-mode, and π-mode. The desired mode for operation in all these three modes is π/2-mode because it is the only unstable mode [Miller *et al.* (1992)]. The proposed variant requires a small external DC magnetic field like a grid-less reltron to ensure the propagation of the electron beams in the oscillator system.

The designing process of any oscillator system starts with some basic parameters such as input beam parameters (i.e. applied beam voltage and beam current), the operating mode of the RF interaction cavity, the desired operating frequency, and finally, the

extraction mode, in which an RF output power is to be extracted. The structural specification of this proposed variant of the reltron oscillator has been calculated using the formulas listed in the Design Methodology section of Chapter-4 and listed in Table 5.1.

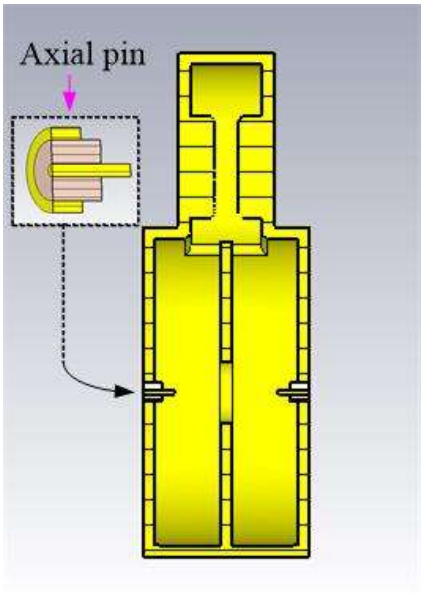

Figure 5.2: 3D schematic view of the RF interaction cavity with coaxial pins.

Kim *et al.* reported a simulation work on a thermionic emission-based reltron oscillator in which they applied a total tube voltage of 920 kV. Of this 920 kV total tube voltage, 120 kV was applied as the cathode voltage and the remaining 800 kV in the post acceleration region. From the simulation results, it was noted that the high voltage DC pulse in the post acceleration region promotes the plasma formation in the device. This plasma formation limits the pulse width of the generated RF signal to 200 ns. The width of the generated RF pulse when compared with the experimentally reported thermionic emission-based reltron, it found that the width of the generated RF pulse is reduced by 25 times [Miller *et al.* (1995), Kim *et al.* (2009)]. Since we have proposed this variant of reltron for higher pulse widths, therefore, keeping this in mind, the total applied tube voltage of the device is kept low.

Table 5.1. Electrical and structural specification of the proposed variant of reltron.

Electrical specification	
Total tube voltage (V_{tube})	500 kV
Structural specification	
Desired operating frequency (f_r)	2.856 GHz
Main cavity radius (r_{mc})	39.00 mm
Coupled cavity radius (r_{cc})	26.00 mm
Idler radius (r_{id})	13.00 mm
Idler length (L_{id})	5.850 mm
Disc hole radius (r_h)	12.60 mm
Disc spacing (d_{opt})	16.50 mm
Anode-cathode separation (d_{AK})	18.15 mm
Drift tube length (d_{dt})	39.00 mm
Extraction cavity length (L_{ext})	18.00 mm
Post-acceleration gap length (L_{PA})	48.00 mm
External Magnetic field (B_z^*)	0.38 Tesla

5.3.1. Cold Test Simulation Results

The effect of structural parameters on the resonating frequency of the RF interaction cavity is just similar to the analysis performed in the structural parametric analysis section in Chapter-4. The EM behavior of the RF interaction cavity (shown in Fig. 5.2) includes the electric field distribution and the resonating frequency associated with the different resonating modes that exist within the RF interaction cavity. Therefore, to know the EM behavior of the RF interaction cavity the structure is firstly designed with the help of structural parameters listed in Table 5.1, and then it is simulated using eigenmode solver and frequency-domain solver of the “CST Studio suite”.

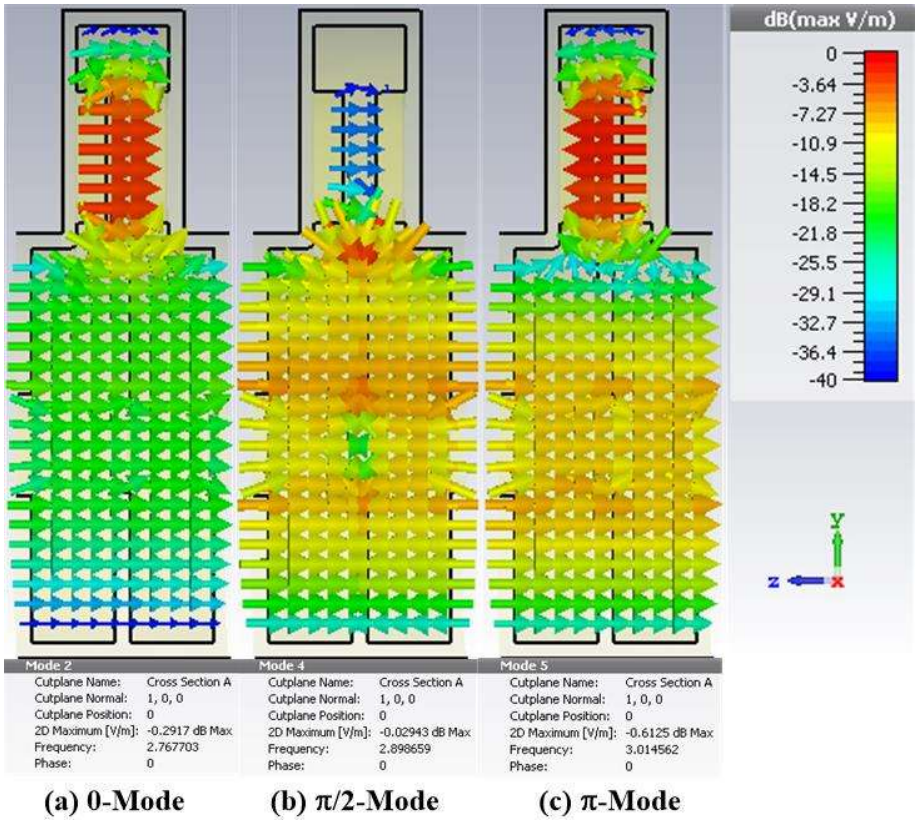

Figure 5.3: The RF electric field distribution inside the RF interaction cavity: (a) 0-mode, (b) π/2-mode, and (c) π-mode.

5.3.1.1. Results of Eigenmode Solver

The electric field distribution associated with the different resonating modes which exist within the RF interaction cavity is obtained by using CST's eigenmode solver. The modeled RF interaction cavity (i.e. SCC) is simulated with the help of an eigenmode solver, and its results are shown in Fig. 5.3. The electric field distribution corresponding to three modes i.e. 0-mode, π/2-mode, and π-mode can be seen in Figs. 5.3 (a), 5.3 (b), and 5.3 (c), respectively. The resonating frequency corresponding to the 0-mode, π/2-mode, and π-mode is 2.76 GHz, 2.89 GHz, and 3.01 GHz, respectively.

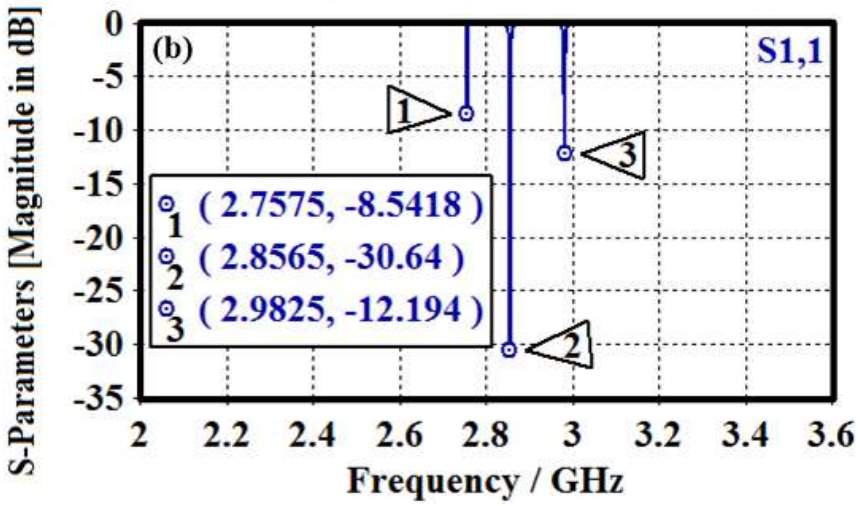

Figure 5.4: Scattering parameter (S_{11}) of the RF interaction cavity.

5.3.1.2. Results of Frequency Domain Solver

After ensuring the establishment of the resonating modes in the RF interaction cavity, the resonating frequency associated with these modes i.e. 0-mode, π/2-mode, and π-mode is obtained by scattering parameter (i.e. S_{11}). Before simulating the RF interaction cavity by the frequency-domain solver, the RF interaction cavity is modeled with two axial pins. These coaxial probes are placed at the front and back end of the main pillbox cavity as shown in Fig. 5.2. The result obtained from the frequency domain solver (i.e. S_{11} the parameter of the RF interaction cavity) is shown in Fig. 5.4. From Fig. 5.4, it is noticed that there are three dips and with every dip, markers are attached. Each dip represents the resonating mode of the RF interaction cavity and the marker shows the resonating frequency associated with that dip. From the figure, it is also noticed that the resonating frequency calculated by the frequency domain solver is nearly equal to the resonating frequency that was predicted by the eigenmode solver.

5.3.2. Hot Test Simulation Results

The RF behavior of the proposed variant is investigated using the PIC solver of the CST. The RF behavior of the device includes the device's conversion efficiency, produced RF strength, RF pulse width, operating frequency, and axial bunching mechanism. The proposed variant of the reltron is designed according to the electrical and structural specifications that are listed in Table 5.1.

Before starting the simulation, an excitation signal of 1500 ns of pulse-width with a rise time of 20 ns is chosen and applied with the help of a discrete port. The discrete port is used to apply a DC voltage at the cathode and post acceleration region. Some inbuilt function such as phase space monitor, waveguide port has also been selected to monitor and stored the axial bunching mechanism and RF growth within the device, respectively. The PIC simulation was carried out for 1500 ns. The kinetic energy distribution of the electron beam is shown in Fig. 5.5., which indicates the axial electron bunching process with respect to the axial direction of the device. The electron bunching does not alter too much when it is compared with the electron bunching at 58 ns (i.e. Fig. 5.5 (a)) and 980 ns (i.e. Fig. 5.5 (a)) which also indicates the stability in generated RF output power.

The amplitude of the generated RF signal is recorded by the waveguide port that is placed at the extraction cavity. Fig. 5.6 to Fig. 5.9 shows the amplitude, operating frequency, and RF output power of the generated RF signal at different applied beam voltage and post acceleration voltage.

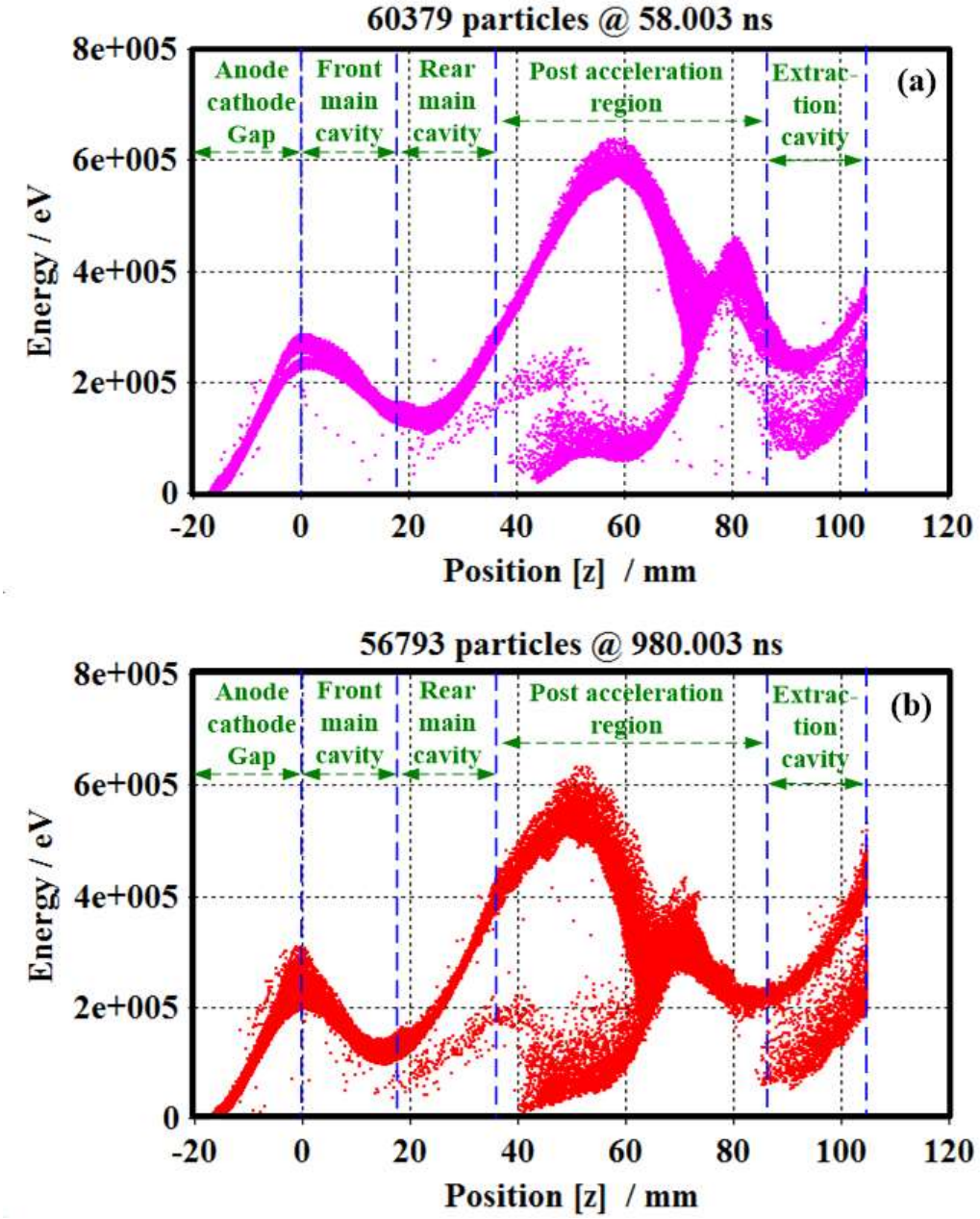

Figure 5.5: Electrons kinetic energy distribution of the electron beam recorded by the inbuilt phase space monitor: (a) axial electron bunching at 58 ns, and (b) axial electron bunching at 980 ns.

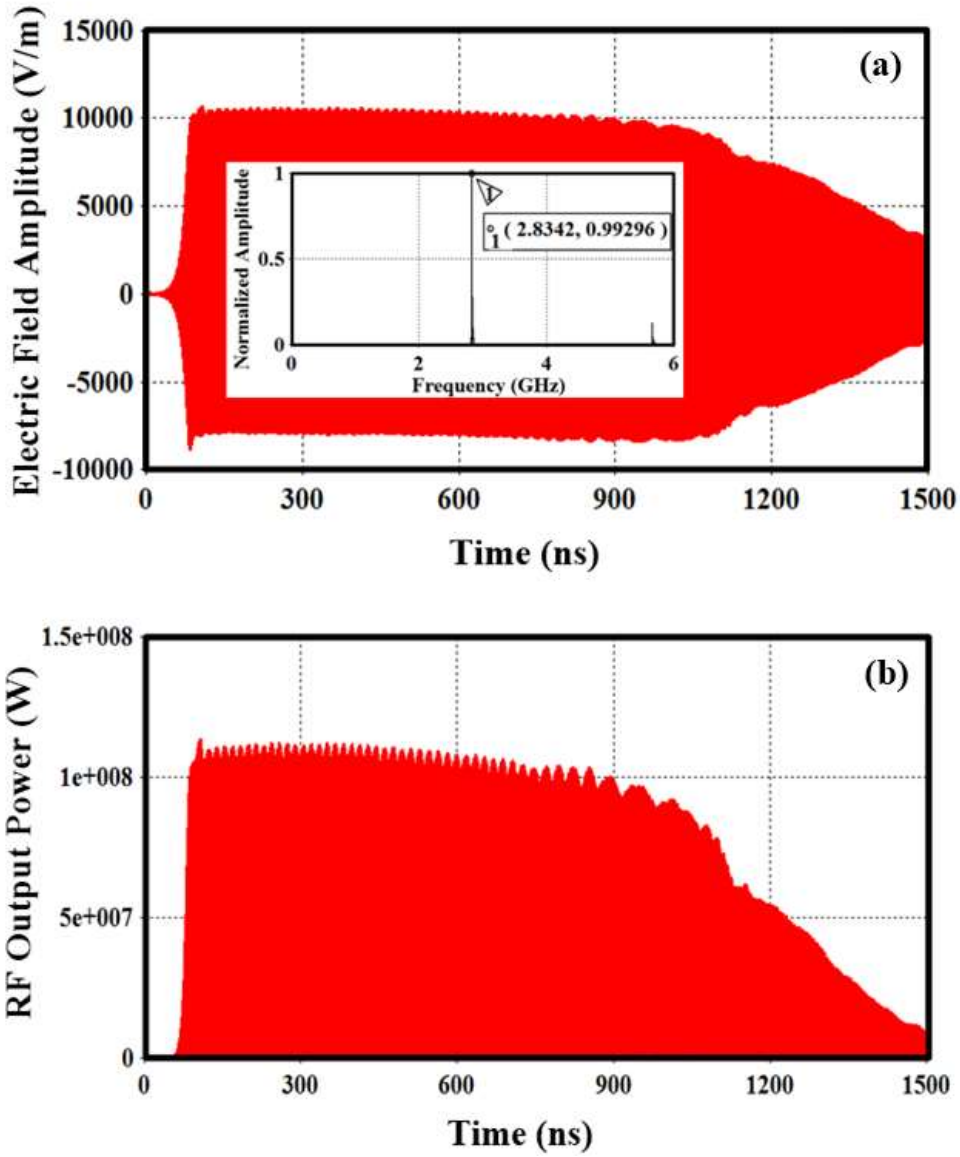

Figure 5.6: Generated RF signal when the applied cathode voltage and post acceleration voltage of 100 kV and 400 kV, respectively: (a) amplitude and operating frequency, and (b) RF output power.

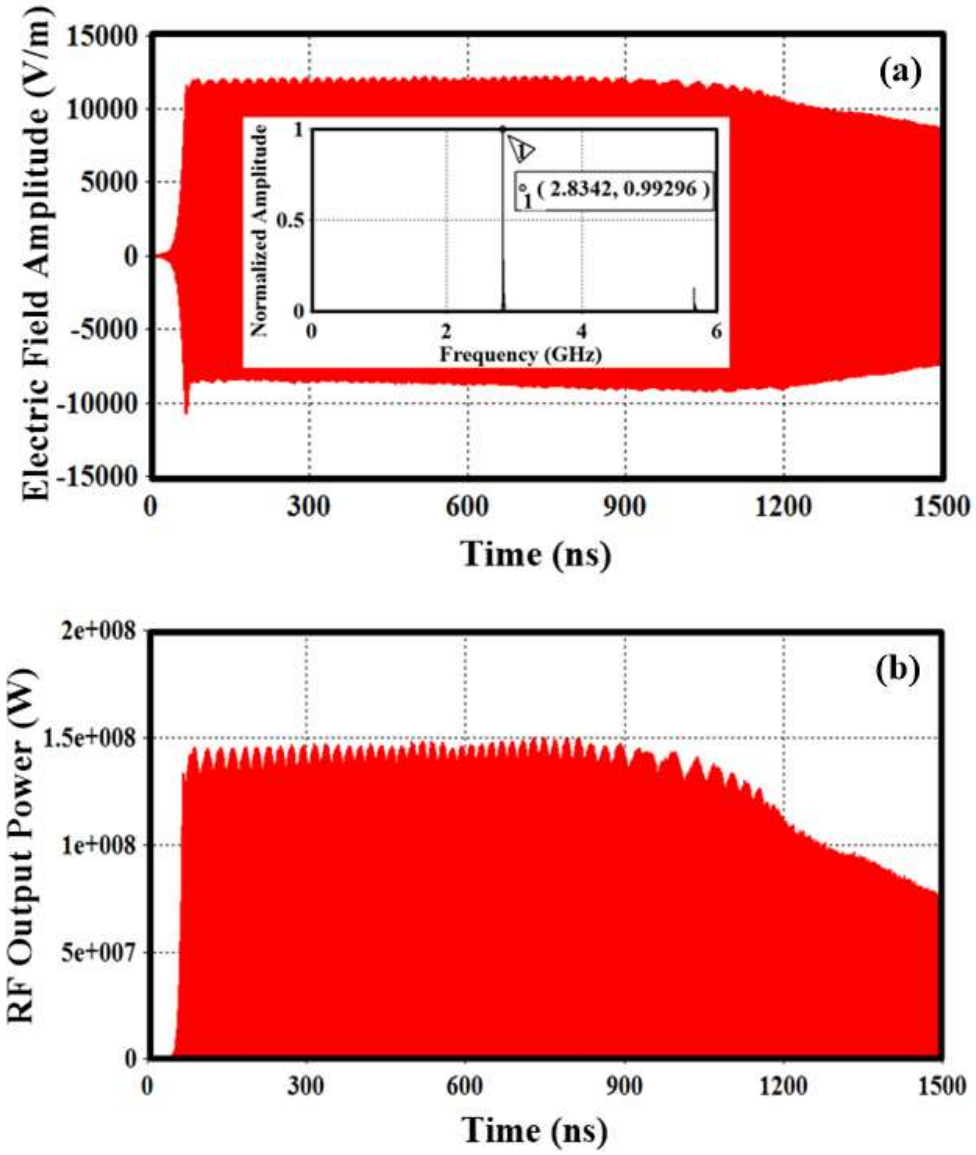

Figure 5.7: Generated RF signal when the applied cathode voltage and post acceleration voltage of 150 kV and 350 kV, respectively: (a) amplitude and operating frequency, and (b) RF output power.

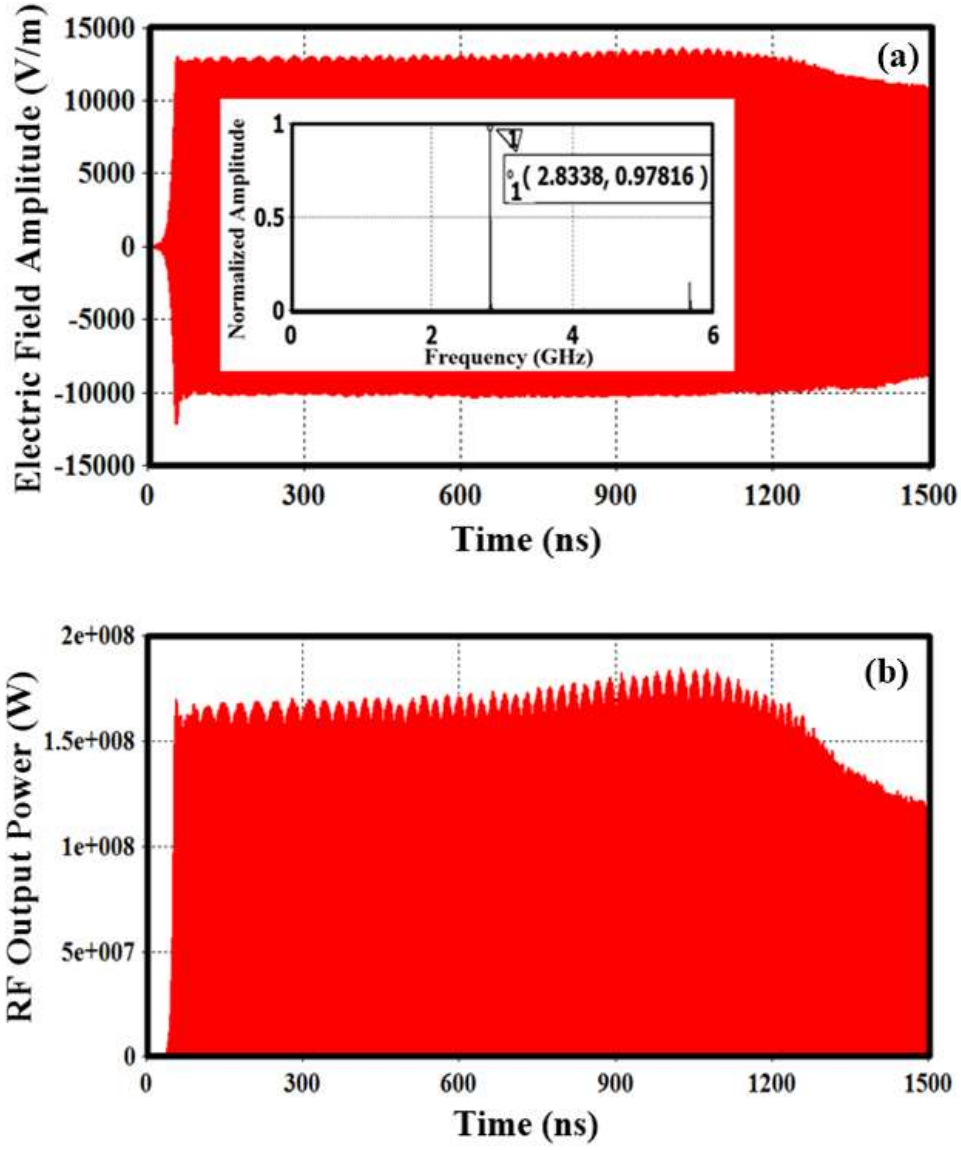

Figure 5.8: Generated RF signal when the applied cathode voltage and post acceleration voltage of 200 kV and 300 kV, respectively: (a) amplitude and operating frequency, and (b) RF output power.

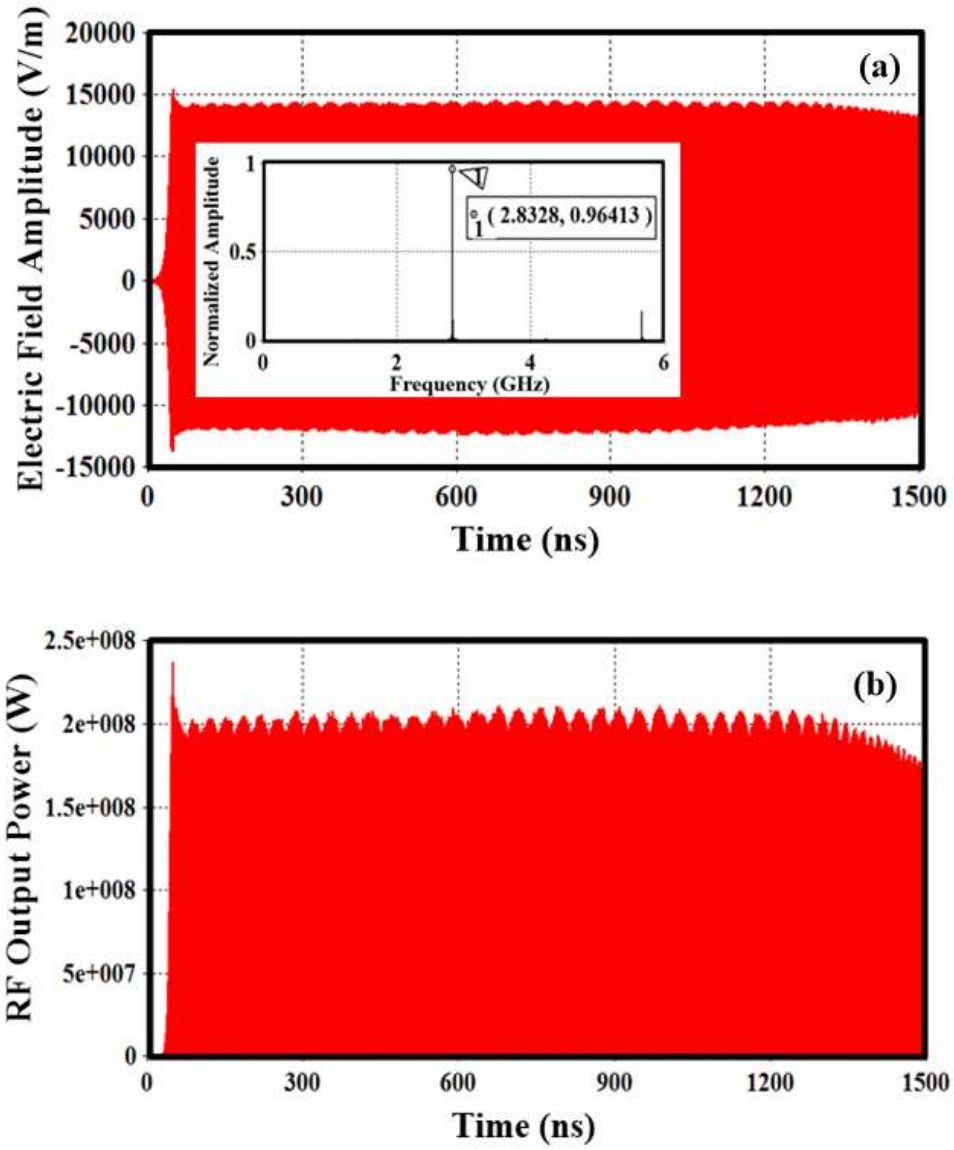

Figure 5.9: Generated RF signal when the applied cathode voltage and post acceleration voltage of 250 kV and 250 kV, respectively: (a) amplitude and operating frequency, and (b) RF output power.

Table 5.2: RF output power and operating frequency at different applied beam and post acceleration voltage.

Applied beam voltage and post-acceleration voltage	**Generated RF Power (MW)**	**Corresponding Figure number which shows the generated RF Power**	**Generated Pulse width (ns)**	**Operating frequency (GHz)**
100 kV & 400 kV	> 100	Fig. 5.6 (b)	> 600	2.8342
150 kV & 350 kV	> 130	Fig. 5.7 (b)	> 950	2.8342
200 kV & 300 kV	> 150	Fig. 5.8 (b)	=1000	2.8338
250 kV & 250 kV	> 190	Fig. 5.9 (b)	=1000	2.8328

For the different applied beam voltage and post acceleration voltage, the corresponding generated RF output power and operating frequency is summarized in Table 5.2. From Fig. 5.6 to Fig. 5.9, it is noticed that the operating frequency is ~22 MHz lower than the resonating frequency which was calculated by the frequency-domain solver. This difference in the frequency is observed due to the phenomena of beam loading.

5.3.2.1. Electrical Parametric Analysis

This analysis has been performed with aim of finding the optimized electrical parameters for the proposed variant of the reltron oscillator. For various electrical parameters such as beam voltage, post acceleration voltage, an applied external DC magnetic field (i.e. B_z^*) the RF behavior of the proposed variant of reltron is investigated. The effect of cathode voltage (i.e. beam voltage), post-acceleration voltage, and applied external magnetic field

on the generated RF power, and pulse-width of the generated RF signal of the proposed variant of reltron oscillator is shown in Fig. 5.10, Fig. 5.11, and Fig. 5.12.

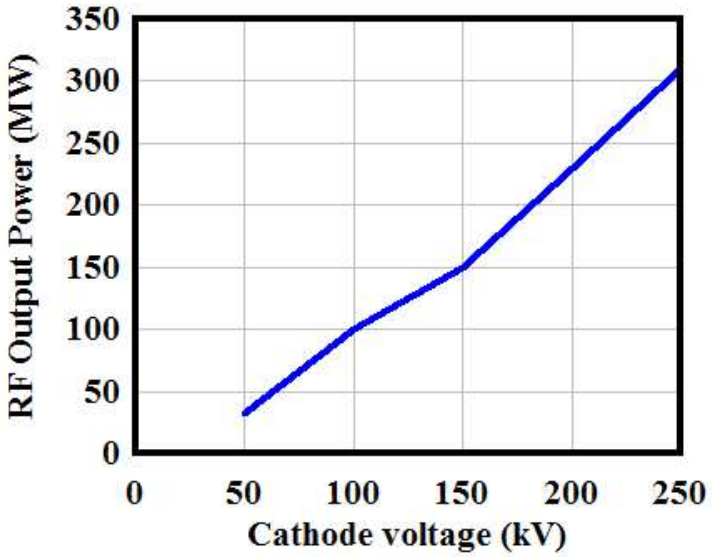

Figure 5.10: RF output power versus cathode voltage (when the applied post acceleration voltage was 400 kV).

From Fig. 5.10, at constant post acceleration voltage, it is noted that the RF output power increases with an increase in applied anode-cathode voltage. The reason behind this increment in the RF output power is: since this device generates its RF output power by converting the kinetic energy of the electron beam. The kinetic energy available for conversion depends directly on the applied anode-cathode voltage (i.e. higher the applied anode-cathode voltage means that higher initial velocity of the electron beam), hence higher the anode-cathode voltage means higher available kinetic energy for conversion i.e. higher RF output power**.** In Fig. 5.11 at constant anode-cathode voltage, it is noted that the RF output power increases with an increase in applied post acceleration voltage. This increase in RF output power occurs because the post acceleration voltage reduces the relative kinetic spread between the electrons in the electron bunches, so the higher the post

acceleration voltage, the lower the relative kinetic spread between electrons [Miller *et al.* (1992)]. In Fig. 5.11 it is also noted that the pulse width of the generated RF signal decreases. This decrease in the pulse width occurs due to the plasma formation which is increases with the applied post acceleration voltage.

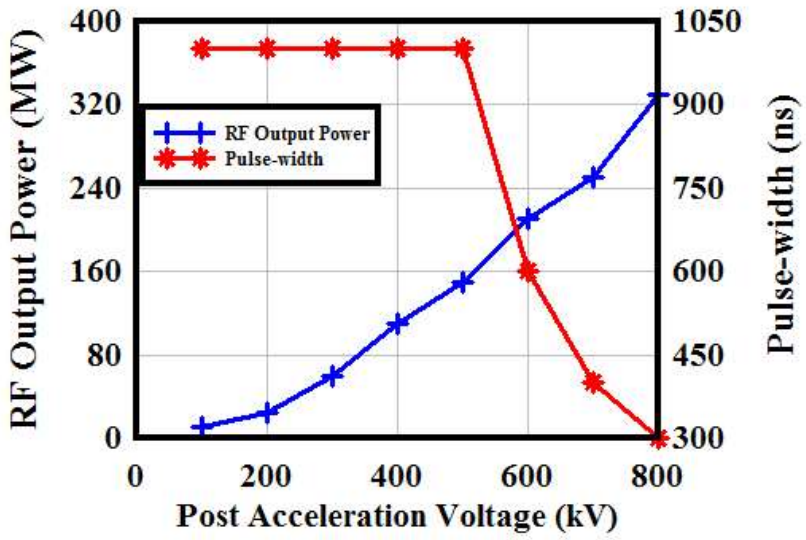

Figure 5.11: RF output power and its pulse-width versus post acceleration voltage (when the applied beam voltage of 100 kV).

In addition, the high post acceleration voltage is responsible for the electric breakdown in the device therefore for long pulse operation the post acceleration voltage should be carefully taken. Fig. 5.12, shows the effect of the applied external applied DC magnetic field on the generated RF output power, and the width of the RF pulse. From the figure, it is noted that the generated RF output power and pulse width become constant after a certain value of the applied external DC magnetic field. The simulation study suggests that the beam conversion efficiency of the proposed device lies in the range of 35-42%.

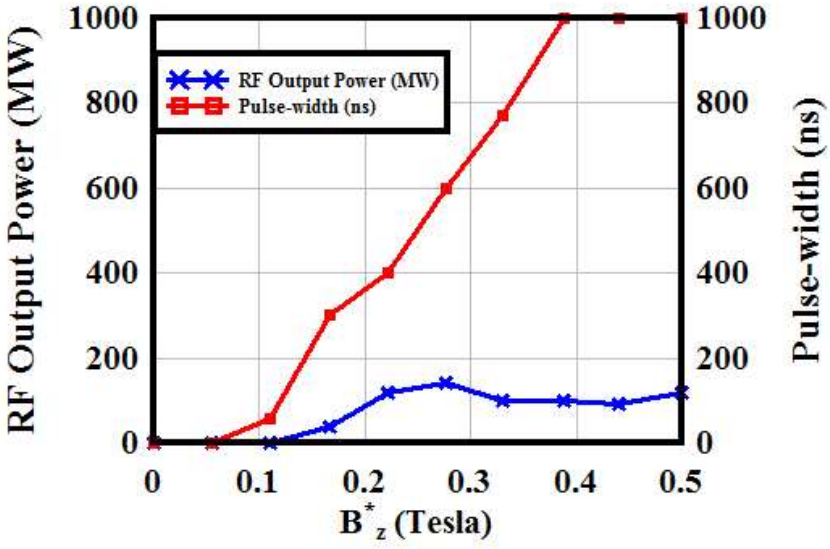

Figure 5.12: RF output power and its pulse-width versus external applied DC magnetic field (when the applied beam voltage and a post acceleration voltage were 100 kV and 400 kV, respectively).

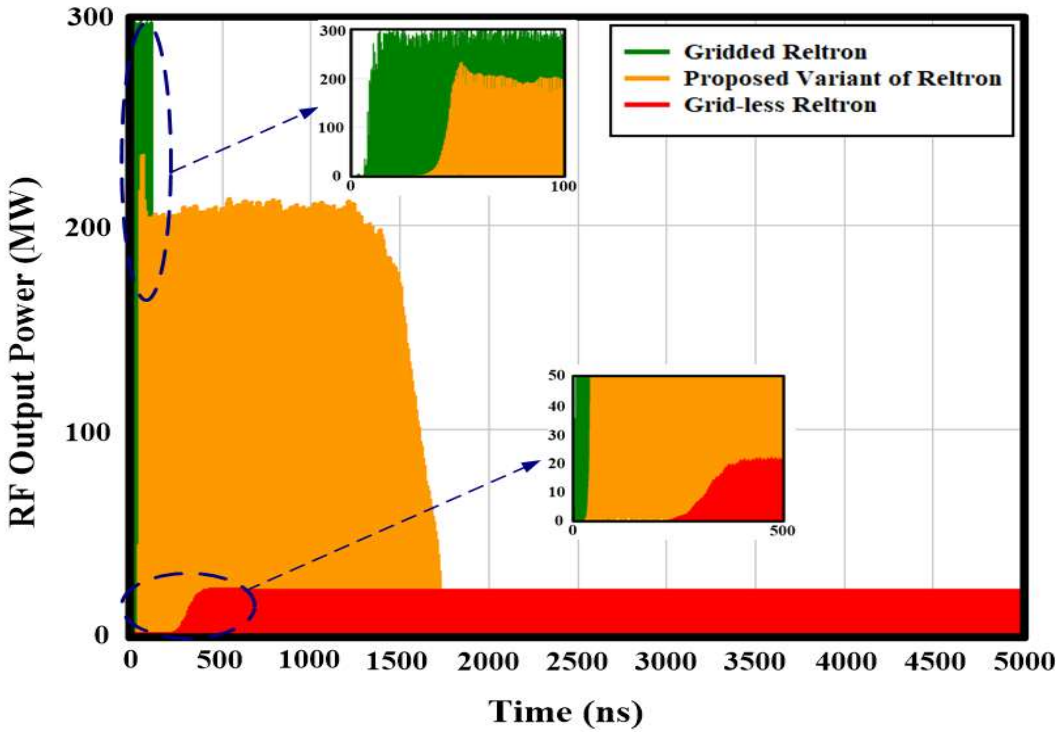

Figure 5.13: Comparison between the generated RF output power and pulse width of the gridded reltron, grid-less reltron, and proposed variant of the reltron.

Fig. 5.13 shows the comparison between the generated RF output power and pulse width of the gridded reltron, grid-less reltron, and proposed variant of the reltron. From the figure, it is noted that the proposed variant of reltron has been capable to produce peak RF power comparable to the gridded reltron while the pulse width is comparable with the grid-less reltron.

5.4. Conclusion

In this chapter, a novel variant of the reltron oscillator i.e. grid-less reltron with explosive emission cathode has been investigated to overcome the problem associated with the gridded reltron (i.e. low RF pulse width, and low PRR) and grid-less reltron (i.e. low RF output power). A comprehensive simulation study has been carried out to analyze the effect of various electrical parameters on the RF performance of the proposed device. Also, the electrical parametric analysis has been performed with aim of finding the optimized electrical parameters for the proposed variant of the reltron oscillator. The simulation study showed that the proposed variant has been capable of producing peak RF power comparable to the gridded reltron while the pulse width is comparable with the grid-less reltron. For operation, the proposed device requires a lower operating voltage, so the probability of plasma formation (which is the main cause of pulse shortening) in the HPM device is greatly reduced and this lower operating voltage also helps in achieving a higher PRR in the device. From this simulation study, the author hopes that the proposed variant meets the demand for such a compact HPM device capable of generating high peak RF power, long RF pulse width, and high repetitive pulse operation.